BIOCHEMISTRY
including biophysical chemistry & molecular biology

Article

pubs.acs.org/biochemistry

Proline in Transmembrane Domain of Type II Protein DPP-IV Governs Its Translocation Behavior through Endoplasmic Reticulum

Kuei-Min Chung,[†] Chih-Hsiang Huang,[†] Jai-Hong Cheng,[†] Cheng-Han Tsai,[†] Ching-Shu Suen,[‡] Ming-Jing Hwang,[‡] and Xin Chen*,[†]

[†]Institute of Biotechnology and Pharmaceutical Research, National Health Research Institutes, Miaoli County 350, Taiwan, ROC

[‡]Institute of Biomedical Sciences, Academia Sinica, Taipei 115, Taiwan, ROC

Supporting Information

ABSTRACT: A transmembrane domain (TMD) at the N-terminus of a membrane protein is a signal sequence that targets the protein to the endoplasmic reticulum (ER) membrane. Proline is found more frequently in TM helices compared to water-soluble helices. To investigate the effects of proline on protein translocation and integration in mammalian cells, we made proline substitutions throughout the TMD of dipeptidyl peptidase IV, a type II membrane protease with a single TMD at its N-terminus. The proteins were expressed and their capacities for targeting and integrating into the membrane were measured in both mammalian cells and *in vitro* translation systems. Three proline substitutions in the central region of the TMD resulted in various defects in membrane targeting and/or integration. The replacement of proline with other amino acids of similar hydrophobicity rescued both the translocation and anchoring defects of all three proline mutants, indicating that conformational change caused by proline is a determining factor. Increasing hydrophobicity of the TMD by replacing other residues with more hydrophobic residues also effectively reversed the translocation and integration defects. Intriguingly, increasing hydrophobicity at the C-terminal end of the TMD rescued much more effectively than it did at the N-terminal end. Thus, the effect of proline on translocation and integration of the TMD is not determined solely by its conformation and hydrophobicity, but also by the location of proline in the TMD, the location of highly hydrophobic residues, and the relative position of the proline to other proline residues in the TMD.

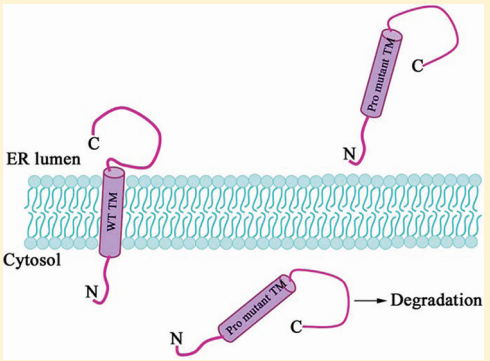

In mammalian cells, one-third of the proteins are secreted or integrated into the plasma membrane. They are often synthesized cotranslationally and translocated through the endoplasmic reticulum (ER) membrane.[1] Signal sequences, including some transmembrane domain (TMD) sequences, target proteins to the ER membrane. When the nascent polypeptide emerges from the ribosome, the signal sequence or the TMD is recognized by the signal recognition particle (SRP). The SRP delivers the ribosome-nascent polypeptide complex to the SRP receptor in the ER membrane and brings the nascent chain into the vicinity of the protein-conducting channel. The channel allows soluble proteins to cross the membrane, and the transmembrane (TM) segments partition to the lipid bilayer, resulting in a membrane-anchored protein. The TMD moves laterally from the center of the pore into the membrane bilayer through an opening formed in the protein-conducting channel.[2,3] This opening is also called the "lateral gate". In support of the "lateral gate hypothesis", during translocation, TM segments can be cross-linked with phospholipid molecules and the protein-conducting channel by chemical photo-cross-linking.[4−6] The partitioning of the TMD to the lipid is a key step in the successful anchoring of membrane proteins.

How TMDs are selected from the translocating polypeptides for partitioning to the lipid bilayer is of fundamental importance in any understanding of protein biogenesis and protein topology. Generally, it is considered to involve a thermodynamic partitioning process that moves the TMD from the hydrophilic environment to the lipid bilayer. Therefore, several hydrophobicity scales have been developed to quantify the insertion of the TM helices into an organic solvent, which mimics the membrane lipid.[7−10] By measuring the insertion efficiency of artificially designed TM segments consisting of only Ala and Leu residues in an *in vitro* transcription/translation system, Hessa et al. quantitatively determined the apparent free energy (ΔG_{app}) for each amino acid at different positions in a TMD.[11,12] They found that the simple addition of ΔG_{app} contributed by an individual amino acid in the TMD explained their insertion behavior.[11,12] This ΔG_{app} scale also correlates well with the hydrophobicity scales for lipid partitioning,[13] further supporting the proposition that TMD

Received: April 20, 2011
Revised: August 11, 2011
Published: August 11, 2011

integration is a partitioning process from the hydrophilic interior of the channel into the lipid bilayer.

Proline is generally not ideal for helix formation. It is frequently found in the TMDs of many integral membrane proteins that function as receptors or transporters.[14,15] For soluble globular proteins, proline is frequently present in the first three positions of the N-terminal parts of α-helices, but it is almost completely absent from the C-terminal or central parts of α-helices.[16,17] Interestingly, for artificially designed TM segments consisting of Ala and Leu residues in an *in vitro* translation system, proline is better tolerated in the N-terminal region than the C-terminal region, independent of TMD orientation in the membrane.[11,18] By making proline substitutions at 15 positions throughout the N-terminal half of the helix B TMD in bacteriorhodopsin, it was found that accommodation to proline substitution depends on its position in the TMD.[19]

It is important to understand how proline in a TMD affects membrane targeting and integration in intact cells. In this study, we used the single TM-containing type II membrane protein dipeptidyl peptidase IV (DPP-IV) as the model substrate and studied the effects of single proline substitution throughout its TMD in mammalian cell culture. DPP-IV is a serine protease and a validated drug target for human type II diabetes.[20] It has a short cytoplasmic tail (amino acids 1−6), a noncleavable TMD (amino acids 7−28), and a catalytic domain located outside the cell (amino acids 29−766) (Figure 2A).[21] The TMD is the targeting signal for the export of DPP-IV through the ER and for its anchoring to the plasma membrane.[21−24] The extracellular domain of DPP-IV is homodimeric.[25,26] Previously, we have shown that dimerization is essential for enzymatic activity. DPP-IV activity is responsible for regulating the half-lives of several important insulin-sensing hormones.[27] The TMD of DPP-IV is dimerized in mammalian cells, which contributes to the optimal activity of DPP-IV.[28] Apart from the functional importance of its enzymatic activity, the interaction between DPP-IV and adenosine deaminase on the cell surface is critical. By recruiting the adenosine deaminase to the plasma membrane, this interaction is important for the regulation of adenosine concentration, adenosine signaling, and the potentiation of T-cell proliferation.[29,30] Thus, both dimerization and cell surface localization are important for the cellular function of DPP-IV. Because its location on the plasma membrane and its catalytic activity are important for its cellular function, proper targeting of DPP-IV to the plasma membrane is important. Here, we expressed the proline mutant proteins both in intact cells and in an *in vitro* translation system and determined the consequent membrane targeting and anchoring capacities of the proteins.

MATERIALS AND METHODS

Plasmid Construction. The expression plasmid pEF-DPP-IV was constructed as described below. The full-length gene encoding DPP-IV was amplified by PCR from a human liver cDNA library with the following primers: 5′-GGATCCATGAAGACACCGTGGAAGGTTC-3′ and 5′-GTCGACCTAAGGTAAAGAGAAACATTGT-3′. The amplified fragment was then ligated into pCR-Blunt II-Topo (Invitrogen). The *Bam*HI/*Sal*I fragment containing DPP-IV was excised from pCR-Blunt II-Topo and ligated into pBluescript-KS (+) (Stratagene) to produce pBluescript-DPP-IV. Mutant full-length DPP-IV constructs were generated as described previously[25,31] using pBluescript-DPP-IV as the template and the primers summarized in Supporting Information Table 1. The wild-type (WT) or mutant DPP-IV fragments were then excised by *Kpn*I digestion, blunt-ended with T4 DNA polymerase, and digested with *Xba*I. The *Xba*I/*Kpn*I (blunted) fragments were then ligated into the expression vector pEF-SCM[32] at the blunted *Xba*I and *Not*I sites.

The plasmids used for *in vitro* transcription were constructed as described below. The full-length genes encoding WT or mutant DPP-IV were amplified by PCR from the expression plasmid pEF-DPP-IV or pEF mutant DPP-IV with the following primers: 5′-CTCATCTCTAGAGCCACCATGAAGACACCGTGGAAGGTTC-3′ and 5′-CACTAGCCCGGGCTATTACTAAGGTAAAGAGAAACATTGTT-3′. The amplified fragments were then digested with *Xba*I and *Sma*I and ligated into pGEM1 (Promega).

The plasmids for the expression of DPP-IV-TMD-containing Lep constructs were constructed as described below. The DPP-IV TMD sequence containing amino acids 7−28 was PCR-amplified from the pEF-DPP-IV plasmid with the following primers: 5′-GTCATCACTAGTGTTCTTCTGGGACTGCTGGG-3′ and 5′-CACTAGGGTACCCAGCAGAACCACGGGCACGG-3′. The amplified fragments were then digested with *Spe*I and *Kpn*I and ligated into pGEM1#2978.str (12) to produce the pGEM1#2978-DPP-IV TM-Lep plasmid. pGEM1#2978.str was a kind gift from Dr. Gunnar von Heijne. Site-directed mutagenesis to introduce mutations into the TMD of DPP-IV was then performed as described previously.

The plasmids used to express the DPP-IV TM-CD13 fusion proteins were constructed as described below. CD13 (amino acids 33−967) was PCR-amplified from a cDNA clone (pCMV-SPORT6 CD13 from Open Biosystems) with the following primers: 5′-GAAGTACTCGAGTTACTCCCAGGAGAAGAACAA-3′ and 5′-CTTATGGATATCTTTGCTGTTTTCTGTGAACCAC-3′. The amplified fragment was then digested with *Xho*I and *Eco*RV and ligated into either pIRES-TM-Flag or pIRES-mutated-TM-Flag to produce pIRES-TM-CD13-Flag, pIRES-TM-L17P-CD13-Flag, pIRES-TM-V18P-CD13-Flag, and pIRES-TM-I20P-CD13-Flag.

Mammalian Cell Culture. Chinese hamster ovary (CHO) and HEK293A cells were purchased from American Type Tissue Culture (ATCC). The HEK293A cells were cultured in complete Dulbecco's modified Eagle's medium (DMEM; Invitrogen), supplemented with 10% fetal bovine serum (FBS; Gibco), 1% nonessential amino acids (Gibco), and 1% penicillin/streptomycin (Gibco). The CHO cells were seeded onto plates and maintained in DMEM/F12 supplemented with 10% FBS and 1% penicillin/streptomycin.

Immunoblotting Analysis and Cell-Surface Biotinylation. To determine the expression of the mutant proteins, HEK293A cells were transfected with the expression plasmids using Lipofectamine 2000, as instructed by the manufacturer (Invitrogen). Forty-eight hours after transfection, the cells were washed twice with phosphate-buffered saline (PBS) and directly lysed on the plates with NP-40 lysis buffer (10 mM HEPES [pH 7.5], 142.5 mM KCl, 5 mM $MgCl_2$, 1 mM EGTA, 0.2% NP-40). The supernatants were collected, and the protein concentrations were determined with the Bradford assay. Total cell lysates (50 μg) were fractionated by sodium dodecyl sulfate−polyacrylamide gel (10%) electrophoresis (SDS-PAGE), transferred to nitrocellulose, and immunoblotted with in-house DPP-IV antibody, which was detected with horseradish-peroxidase-conjugated goat anti-rabbit secondary

antibody (Jackson) and enhanced chemiluminescence (Millipore). To determine whether DPP-IV was located on the plasma membrane, *N*-hydroxysulfosuccinimidobiotin (Pierce), a reagent that modifies amino groups and is considered to be membrane-impermeable, was used.[33] Biotinylation and detection were performed as previously described.[34]

Immunoprecipitation of [^{35}S]-Labeled DPP-IV Proteins. To detect the proteins, a radiolabeling experiment was performed as previously described.[35] CHO cells transfected with pEF plasmids were starved in Cys/Met-free DMEM for 1.5 h before they were labeled with 100 μCi of [^{35}S]-Cys/Met (PerkinElmer) for 30 min at 37 °C. Immediately after labeling, the cells were washed once with cold PBS, pelleted, and lysed with lysis buffer (50 mM Tris-HCl [pH 7.4], 150 mM NaCl, 1 mM EDTA, 1% Triton X-100) containing protease inhibitors. The radiolabeled DPP-IV proteins in the cell lysate were immunoprecipitated with in-house anti-DPP-IV antibody and separated by SDS-PAGE (8%). The radioactive proteins were visualized with autoradiography.

Quantitative RT-PCR. Quantitative RT-PCR was performed according to a published protocol.[36] The RNA from each cell line examined was extracted with TRI Reagent (Molecular Research Center, Cincinnati, OH), according to the manufacturer's instructions. The RNA was converted to cDNA with ImProm-II Reverse Transcriptase (Promega), and quantitative PCR was performed with the ABI Prism 7900 Sequence Detection System using SYBR Green PCR Master Mix (ABI). The sequences of the primers used for the quantitative PCR were 5′-GTGACATGCCTCAGTTGTGAGC-3′ and 5′-TGGAGGGCATCTGGACATTC-3′ for DPP-IV and 5′-GAAGGTGAAGGTCGGAGTCA-3′ and 5′-TGGAAGATGGTGATGGGATT-3′ for glyceraldehyde-3-phosphate dehydrogenase (GAPDH) cDNA. The threshold cycle (Ct) for DPP-IV was calculated with a normalization constant relative to the amplification of GAPDH cDNA, as described previously.[36]

***In Vitro* Translocation Assay and Protease K Assay.** An *in vitro* translocation assay was also performed using the TNT Quick Coupled Reticulocyte Lysate System (Promega). The translation mix (25 μL) contained 1 μg of pGEM1 plasmid, 20 μL of TNT mixture, 20 μCi of [^{35}S]-methionine (PerkinElmer), and 2 μL of canine pancreatic microsomes (Promega). *In vitro* transcription and translation were performed in the TNT Coupled Wheat Germ Extract System (Promega), as described previously.[34,37] The translation mix (50 μL) contained 1 μg of pGEM1 plasmid, 25 μL of TNT wheat-germ extract, 2 μL of TNT reaction buffer, 0.5 μL of 1 mM amino acid mixture (minus methionine), 20 μCi of [^{35}S]-methionine (PerkinElmer), and 40 U of RNasin ribonuclease inhibitor (Promega). The samples were incubated at 30 °C for 90 min and then analyzed on a NuPAGE 4%-12% Tris−glycine gradient gel (Invitrogen).

The samples were treated with proteinase K (0.05 mg/mL) on ice for 8 min, and the reaction was terminated with 2 mM phenylmethylsulfonyl fluoride. For alkaline extraction, the translation product was diluted 10-fold by volume with 0.1 M sodium carbonate (pH 12.5) and kept on ice for 30 min. The membrane-associated polypeptides were separated from those not anchored to the membrane by centrifugation at 82 000 rpm in a Beckman 120.2 rotor for 10 min.

***In Vivo* Alkaline Extraction Assay.** For *in vivo* alkaline extraction, cells were homogenized by passage through a 29G needle in a low salt buffer (50 mM HEPES [pH 7.4], 10 mM potassium chloride, 1.5 mM magnesium acetate and protease inhibitor cocktail (Roche)). Cell extracts were then centrifuged at 3000*g* for 10 min, and the supernatant fractions were centrifuged at 100000*g* for 10 min. The resulting membrane pellet was washed with HKM buffer (25 mM HEPES [pH 7.4], 125 mM potassium acetate, 5 mM magnesium acetate), then dissolved in 0.1 M sodium carbonate at pH 12.5, and kept on ice for 30 min. The membrane-associated polypeptides were separated from those not anchored in the membrane by centrifugation at 100000*g* in a Beckman 120.2 rotor for 10 min. After centrifugation, the pellet contained the membrane-associated polypeptides and the nonanchored proteins were recovered in the supernatant.

RESULTS

Position Effect of Proline on Membrane Integration of Proteins in Mammalian Cells. To investigate the membrane targeting and integration of DPP-IV, a TMD-less DPP-IV (deletion of amino acids 2−38) was constructed and expressed in CHO cells, which do not express DPP-IV endogenously. Without the TMD, the mutant DPP-IV is expected to localize in the cytosol. Interestingly, no mutant proteins were found in total cell lysates by immunoblotting analysis (Figure 1A, lane 3).

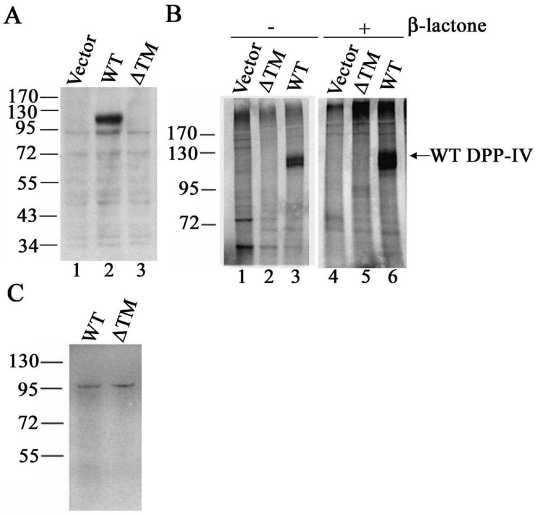

Figure 1. TMD-less DPP-IV was degraded in the cytosol. (A) Cells were transfected with plasmids encoding the following mutations: (1) vector only, (2) WT, or (3) ΔTM, and the cell lysates were subjected to immunoblotting analysis with anti-DPP-IV antibody. (B) HEK293A cells were labeled with [^{35}S]-Cys/Met, and their proteins were then immunoprecipitated. Lanes 1−3 contain the proteins from cells transfected with plasmids encoding the following sequences: (1) vector, or (2) WT, or (3) ΔTM. Lanes 4−6 are the identical, except that the proteasome inhibitor β-lactone was added (50 μM). The radioactive proteins were detected by autoradiography. (C) Protein expression was detected in an *in vitro* translation assay in wheat-germ lysates with plasmids encoding the following sequences: (1) WT or (2) ΔTM. The radioactive proteins were detected by autoradiography.

In controls, WT DPP-IV was expressed normally (Figure 1A, lane 2, and Figure 1B, lanes 3 and 6). In the presence of the proteasomal inhibitor β-lactone, TMD-less DPP-IV was not detected (Figure 1B, lane 5), suggesting that the mutant protein was degraded while still being synthesized. The failure of detection was not attributable to a defect in either the

transcription or translation process because the TMD-less proteins were readily detected in the *in vitro* transcription and translation system with wheat-germ lysates (Figure 1C, lane 2), similar to the WT DPP-IV (Figure 1C, lane 1). Therefore, DPP-IV proteins without TMDs were not targeted to the ER membrane. Failure of the DPP-IV protein to target to the ER membrane would result in the proteins being expressed in the cytosol, followed by their degradation.

To understand the effects of proline on membrane targeting and integration in mammalian cells, we introduced single proline substitutions into the DPP-IV TMD from position 10 to 23 (Figure 2A). WT DPP-IV TMD contains a proline at position 24. The mutant proteins were expressed in HEK293A or CHO cells and were detected by immunoblot. Neither cell line expresses DPP-IV endogenously. Interestingly, the L17P, V18P, and I20P mutant proteins were not detected in the total cell lysates by immunoblot (Figure 2B, lanes 10, 11, and 13), whereas other mutant proteins were expressed at WT levels (Figure 2B). The expressed proteins were localized to the plasma membrane, as detected by cell-surface biotin labeling followed by immunoprecipitation (Supporting Information Figure 1A). In this experiment, the insulin receptor on the cell surface and the actin in the cytoplasm were used as controls for protein localization (Supporting Information Figure 1A). The mutant proteins also maintained their dimeric structures, as shown by nonreducing gel electrophoresis (Supporting Information Figure 1B). The most severe effects were associated with proline substitutions at the central part of the DPP-IV TMD (i.e., L17P, V18P, and I20P).

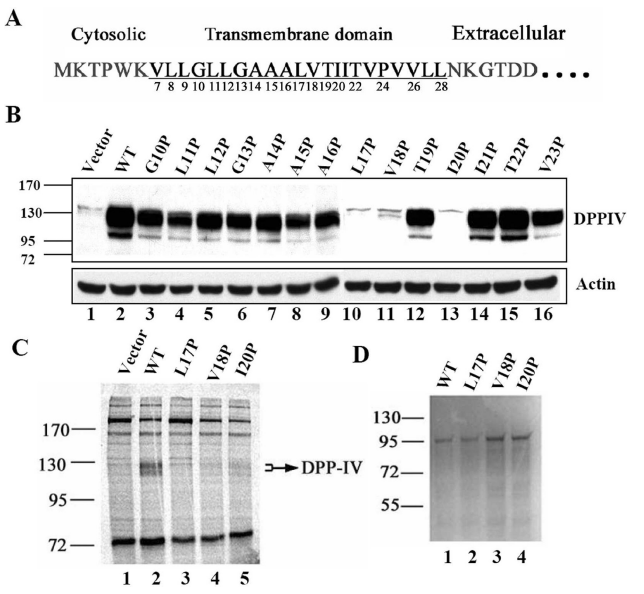

Figure 2. Membrane anchoring mediated by proline-containing TMDs. (A) The sequence of the human DPP-IV TMD is underlined. (B) HEK293A cells were transfected with plasmids encoding the following TMD mutations: (1) vector only, (2) WT, (3) G10P, (4) L11P, (5) L12P, (6) G13P, (7) A14P, (8) A15P, (9) A16P, (10) L17P, (11) V18P, (12) T19P, (13) I20P, (14) I21P, (15) T22P, or (16) V23P. Then, immunoblotting analysis with anti-DPP-IV antibody was performed. (C) Lanes 1−5 contain the proteins from HEK293A cells transfected with the following plasmids: (1) vector only, (2) WT, (3) L17P, (4) V18P, or (5) I20P. DPP-IV protein expression was detected by [^{35}S]-labeling in HEK293A cells followed by immunoprecipitation. The radioactive proteins were detected by autoradiography. (D) The proteins were detected with an *in vitro* translation assay in wheat-germ lysates after expression from plasmids encoding the following mutations: (1) WT, (2) L17P, (3) V18P, or (4) I20P. The radioactive proteins were detected by autoradiography.

The mutant proteins L17P, V18P, and I20P were not detected after the cells were labeled with [^{35}S]-Met and immunoprecipitated with an anti-DPP-IV antibody (data not shown). Moreover, they were not detected after the addition of the proteasome inhibitor β-lactone (Figure 2C, lanes 3−5). We used quantitative PCR to confirm that this failure to detect the L17P, V18P, and I20P proteins was not due to transcriptional defects associated with the mutations (data not shown). Furthermore, the full-length mutant DPP-IV proteins were detected at the expected molecular masses after *in vitro* translation in wheat-germ lysates (Figure 2D), indicating that the translational process was not affected by any of these TMD mutations. Because these three mutant proteins were not detectable in the total cell lysates, they were either mistargeted to the cytosol and degraded or mistargeted extracellularly without being anchored to the plasma membrane by their TMDs.

Targeting and Integration Defects of the Proline Mutants. These mutant proteins might have eluded detection in total cell lysates because they were secreted to the extracellular milieu. To investigate this hypothesis, we concentrated the cell media and analyzed them with immunoblotting. As controls, residual amount of WT DPP-IV was found in the medium (Figure 3A, lane 2), probably due to shedding. As

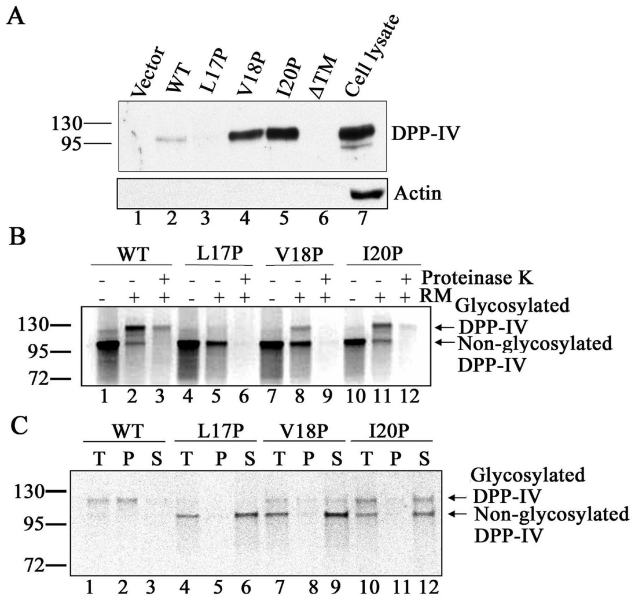

Figure 3. Proline-substitution TMDs defective in either protein translocation and membrane anchoring. (A) Cells were transfected with plasmids encoding the following mutations: (1) vector only, (2) WT, (3) L17P, (4) V18P, (5) I20P, or (6) ΔTM. ΔTM is the truncation of the TMD from aa 2−38. The culture medium were collected and concentrated, and then the DPP-IV proteins were detected with immunoblotting analysis. Lane 7 shows the total cell lysates from cells transfected with the WT plasmid. (B) *In vitro* translation of the mutant DPP-IVs in a rabbit reticulocyte lysate system was performed in the presence or absence of rough microsomes (RM). Proteolysis with proteinase K was performed where indicated. The radioactive proteins were detected by autoradiography. (C) T indicates the *in vitro* translation products in the reticulocyte lysates in the presence of rough microsomes (RM). Pellet (P) and supernatant (S) are the fractions produced by alkaline extraction. The radioactive proteins were detected by autoradiography.

expected, no TMD-less DPP-IV was detected (Figure 3A, lane 6). V18P and I20P were secreted to their media (Figure 3A, lanes 4 and 5), whereas no L17P protein was detected in the medium (Figure 3A, lane 3). These results suggest that the V18P and I20P mutations did not affect the ER targeting function of the TMDs, but they failed to anchor the proteins to the membrane. Similar to TMD-less DPP-IV, the L17P mutation failed to target the proteins to the membrane, resulting in its degradation in the cytosol.

To confirm these observations, an *in vitro* translation assay of the reticulocyte lysates was performed. In the absence of microsomes/ER, only the non-glycosylated forms of DPP-IV proteins were detected for WT and all mutant proteins (Figure 3B, lanes 1, 4, 7, and 10). In the presence of microsomes/ER, WT DPP-IV was glycosylated (Figure 3B, lane 2). Glycosylated WT DPP-IV was found in the pellet, and it was integrated into the membrane, as determined by alkaline extraction (Figure 3C, lane 2). With microsomes/ER, both the glycosylated and non-glycosylated forms of V18P and I20P were detected (Figure 3B, lanes 8 and 11), whereas only the non-glycosylated form of L17P was detected (Figure 3B, lane 5). The non-glycosylated forms of the proteins were degraded upon protease K treatment (Figure 3B, lanes 3, 6, 9, and 12), indicating that they were not translocated to the ER. The glycosylated and non-glycosylated mutant proteins were all extractable by alkaline treatment, indicating that they were not integrated into the membrane (Figure 3C, lanes 6, 9, and 12). These results are consistent with those from the mammalian cell cultures. The TMDs of V18P and I20P failed to anchor the proteins to the membrane, but they still properly targeted the proteins to the ER. The TMD of L17P completely failed to target the protein to the ER, resulting in its degradation in the cytosol.

Membrane Targeting and Integration Mediated by Proline Conformation and Hydrophobicity. To determine whether the translocation and integration defect is associated with the conformation of proline in the TMD, we replaced proline with amino acids with similar capacities for membrane integration, such as Asn (N), Gln (Q), and His (H).[11,12] On the basis of the ΔG_{app} scale, these substitutions should not rescue the translocation and integration defects of the proteins (Supporting Information Figure 2). Expression of the proteins was assessed in mammalian cells by immunoblotting total cell lysates. As shown in Figure 4, mutant proteins with N/Q/H substitutions at L17, V18, and I20 were detectable, suggesting that they were translocated to the ER (Figure 4A,C,E, lanes 4, 5, and 6, compared to lane 3). The mutant proteins were anchored to the membrane, as confirmed by alkaline extraction (Figure 5A–C). Among these mutant proteins, the V18N, V18Q, and V18H proteins were also secreted into the culture medium (Figure 4D, lanes 4–6), indicating that these mutations were partially defective in membrane anchoring. Therefore, proline mutational defects could be rescued by substitutions with other amino acids of similar hydrophobicity. Conformation of proline, other than hydrophobicity, is the factor responsible for the translocation and integration defects of TMDs.

Based on the ΔG_{app} scale for membrane integration, Gly (G) and Thr (T) are slightly more hydrophobic than proline and should favor the membrane integration of TMDs.[11,12] Gly is a known helix breaker in soluble helices. Thr is found in proline-kinked TM helices at a slightly higher frequency than other residues,[38,39] and it can modulate the conformation of proline-kinked

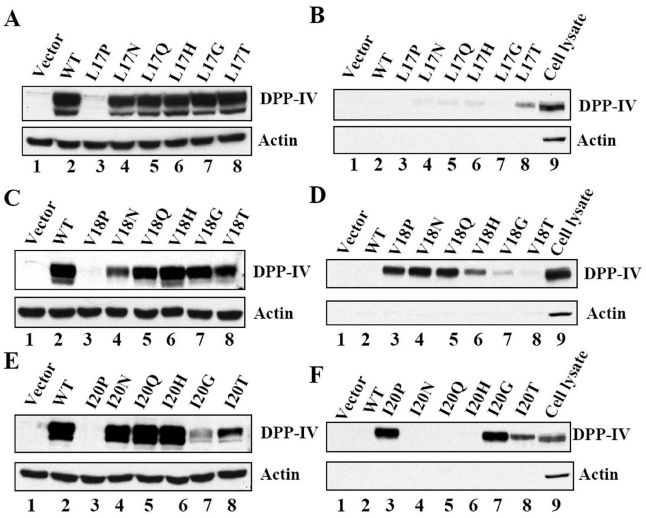

Figure 4. Hydrophobicity is not the determining factor critical for membrane targeting and anchoring. HEK293A cells were transfected with plasmids, and the expression of the proteins was detected by immunoblotting analysis. The plasmids encoding mutations in which L17, V18, and I20 substituted with P, N, Q, H, G, or T are indicated above each lane. In panels A, C, and E, the total cell lysates were collected for immunoblotting analysis. In panels B, D, and F, the culture medium were collected for immunoblotting analysis. Lane 9 is the control: the total cell lysates from cells transfected with the WT plasmid. In panels A and B, the cells were transfected with plasmids encoding the following mutations: (1) vector only, (2) WT, (3) L17P, (4) L17N, (5) L17Q, (6) L17H, (7) L17G, or (8) L17T. In panels C and D, the cells were transfected with plasmids encoding the following mutations: (1) vector only, (2) WT, (3) V18P, (4) V18N, (5) V18Q, (6) V18H, (7) V18G, or (8) V18T. In panels E and F, the cells were transfected with plasmids encoding the following mutations: (1) vector only, (2) WT, (3) I20P, (4) I20N, (5) I20Q, (6) I20H, (7) I20G, or (8) I20T.

TM helices.[38,39] Except for I20G (Figure 4E, lane 7), proteins with Gly or Thr substitutions at positions 17, 18, or 20 were detectable in total cell lysates (Figure 4A,C,E, lanes 7 and 8), and they were integrated into the membrane, as confirmed by alkaline extraction (Figure 5A–C). Conversely, some I20G and I20T proteins were secreted extracellularly (Figure 4F, lanes 7 and 8). Thus, proline at these positions does not favor its successful translocation; the conformation of proline imposes an obstacle for membrane integration.

Rescue of Translocation and Integration Defects by the P24A Mutation. The TMD of DPP-IV contains another proline residue at position 24, P24 (Figure 2A). By mutating P24 to Ala (P24A), we investigated whether the relative positions of the two proline residues are also factors contributing to the membrane anchoring defect. Proline mutant proteins with P24A mutations were detected in total cell lysates, and they were anchored to the membrane, as determined by alkaline extraction, indicating a rescue of the translocation and integration defects of the L17P and V18P mutants (Figure 5D and Figure 6A, lanes 6 and 7). The results further supported the proposition that the conformation of the TMD afforded by proline has significant negative effects on TMD translocation and anchoring. The I20P/P24A mutant was predominantly found in the medium rather than anchored to the membrane (Figure 6B, lane 5), suggesting that proline

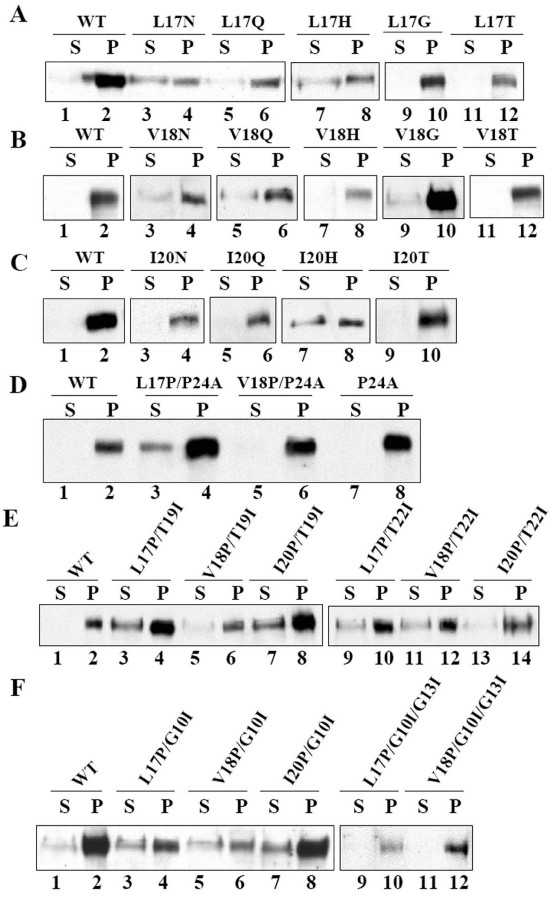

Figure 5. Membrane anchoring of DPP-IV TMD mutants. HEK293A cells were transfected with plasmids encoding the DPP-IV TMD mutations, and alkaline extraction was used to localize the proteins to either the pellet (P) or the supernatant (S). The mutation site in the DPP-IV TMD is indicated on the top of each lane.

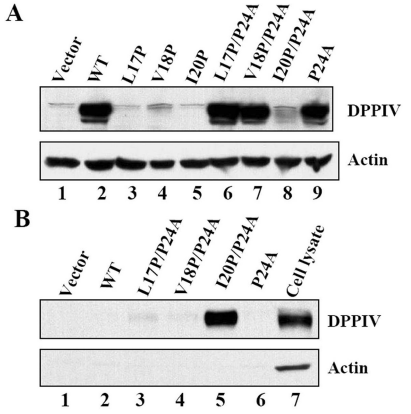

Figure 6. P24A mutation rescues the translocational and anchoring defects. (A) HEK293A cells were transfected with plasmids encoding the following mutations: (1) vector only, (2) WT, (3) L17P, (4) V18P (5) I20P, (6) L17P/P24A, (7) V18P/P24A, (8) I20P/P24A, or (9) P24A, followed by immunoblotting analysis with anti-DPP-IV antibody. (B) The culture medium was collected for immunoblotting analysis with anti-DPP-IV antibody.

substitution in the central and C-terminal regions of the TMD has a greater impact on membrane anchoring.

Rescue of Translocation and Integration Defects by Increasing Hydrophobicity. To investigate whether an increase in TMD hydrophobicity would improve the translocation and anchoring of DPP-IV, we substituted Gly10, Gly13, Thr19, or Thr21 with isoleucine (Ile, I), a highly hydrophobic residue. The mutant proteins were expressed in HEK293A cells and detected by immunoblotting analysis with total cell extracts. The T19I and T22I mutant proteins were detected, and they were glycosylated (Figure 7A), indicating

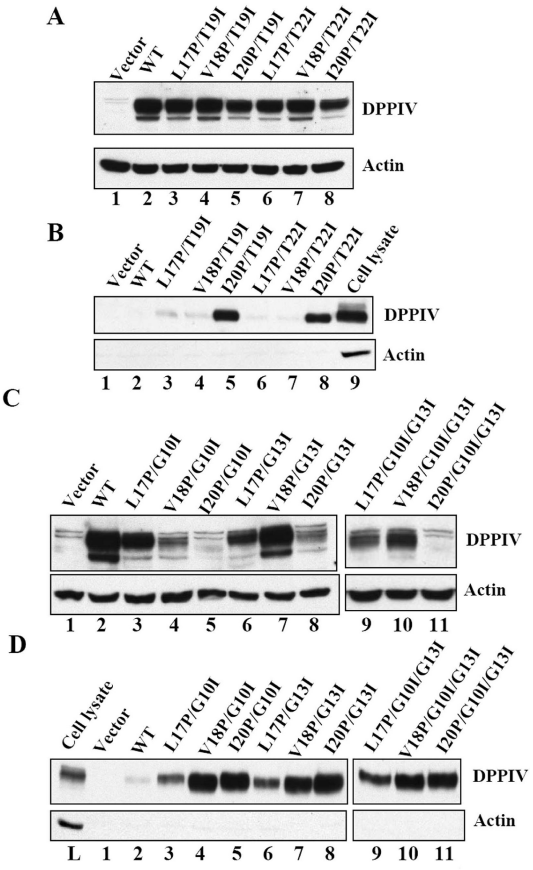

Figure 7. Increasing hydrophobicity rescues the membrane targeting and anchoring defects. The mutation generated is indicated on the top of each lane. Panels A and C are total cell lysates, and panels B and D are concentrated culture medium. Lane L is the control: total cell lysates from cells transfected with the WT plasmid. (A, B) The T19I and T22I mutations, respectively, were introduced into the proline mutants. The cells were transfected with plasmids encoding the following mutations: (1) vector only, (2) WT, (3) L17P/T19I, (4) V18P/T19I, (5) I20P/T19I, (6) L17P/T22I, (7) V18P/T22I, or (8) I20P/T22I. (C, D) The G10I and G13I mutations, respectively, were introduced into the proline mutants. The cells were transfected with plasmids encoding the following mutations: (1) vector only, (2) WT, (3) L17P/G10I, (4) V18P/G10I, (5) I20P/G10I, (6) L17P/G13I, (7) V18P/G13I, (8) I20P/G13I, (9) L17P/G10I/G13I, (10) V18P/G10I/G13I, or (11) I20P/G10I/G13I.

that the proteins were successfully translocated into the ER. Single mutation T19I or T21I mutants rescued the translocation and anchor defects of all three proline mutants, as confirmed by alkaline extraction coupled with membrane fractionation (Figure 5E and Figure 7A, lanes 3–8). Some I20P/T19I and I20P/T22I mutant proteins were also detected in the media (Figure 7B, lanes 5 and 8), indicating partial

dx.doi.org/10.1021/bi200605h | Biochemistry 2011, 50, 7909–7918

anchoring defects associated with these mutations. In comparison, all G10I or G13I mutants were detected in the culture media (Figure 7D, lanes 3–8). Some L17P/G10I, L17P/G13I, and V18P/G13I mutant proteins were anchored to the membrane (Figure 7C, lanes 3, 6, and 7), whereas a majority of V18P/G10I, I20P/G10I, and I20P/G13I mutant proteins were not anchored to the membrane (Figure 7C, lanes 4, 5, and 8).

In light of the weaker capacity of G10I or G13I to rescue the translocation and anchoring defects, we next asked whether G10I/G13I double substitutions would increase the anchoring capacity of the TMD. Interestingly, all of these mutants were secreted into the media (Figure 7D, lanes 9–11). The triple mutant G10I/G13I/I20P still did not anchor the TMD to the membrane (Figure 7D, lane 11). Thus, compared to L17P and V18P, I20P still had the most severe defects, even upon increasing the hydrophobicity of the TMDs with G10I/G13I substitutions. T19I or T22I substitutions were much more effective in rescuing the defects imposed by proline, suggesting that increasing hydrophobicity at the central and C-terminal part of the TMD has a much greater impact on overcoming the negative impact on membrane targeting and integration than equivalent changes in the N-terminal region.

Defects of Translocation and Integration Are Independent of the Extracellular Domain. To investigate whether the extracellular C-terminal domain of DPP-IV affects ER translocation, the TMD of DPP-IV (amino acids 1–40) was fused to the extracellular domain of CD13 (amino acids 33–967) and was expressed in HEK293A cells. Like DPP-IV, CD13 is a type II membrane protease with a single TMD at the amino terminus. The glycosylated CD13 fusion protein was readily detected both in the total cell extract (Figure 8A, lane 2) and in the culture medium (Figure 8B, lane 2). WT-CD13 was secreted, indicating that the extracellular domain or regions outside the DPP-IV TMD weakened its anchoring capacity. L17P-CD13 was not found either in the culture media (Figure 8B, lane 3) or at the cell surface (Figure 8C, lane 3), and a tiny amount of the non-glycosylated form was found in the total cell lysates (Figure 8A, lanes 3 vs 7), indicating that L17P-CD13 was located in the cytosol and not translocated into ER. Thus, L17P TMD remained incapable of targeting a different cargo into the ER. Both the V18P and I20P-CD13 fusions behaved like their DPP-IV counterparts by being predominantly secreted into the media (Figure 8B). Thus, for mutant TMDs, TMD-mediated translocation is independent of the cargo proteins they carry.

Similar to the results from the cell culture (Figure 8A–C), glycosylated WT-CD13 proteins were detected in the *in vitro* translation assay. They were not degraded by proteinase K, indicating that they were translocated into the microsome (Figure 8D, lanes 2 and 3). Non-glycosylated TMD mutant-CD13 fusions were all degraded by protease K treatment, indicating that they were not translocated into the microsomes (Figure 8D, lanes 6, 9, and 12). L17P was not glycosylated in the *in vitro* translation assay (Figure 8D, lane 5), suggesting that L17P still could not mediate translocation to the ER when fused to a different extracellular domain. Combined with what we observed with full length DPP-IV (Figures 2 and 3), the results here indicate that for the mutant proteins TMD-mediated translocation is independent of the cargo proteins they carry.

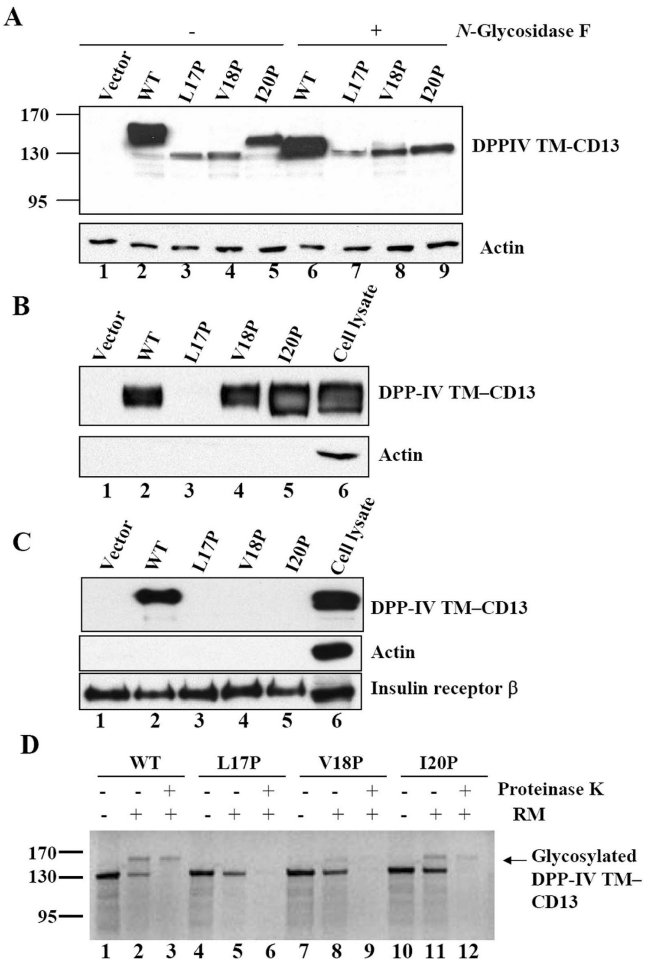

Figure 8. Translocational and anchoring defects of proline mutants are independent of extracellular domain. (A) The extracellular domain of CD13 was fused after the TMD of DPP-IV, and the plasmid was expressed in HEK293A cells, followed by immunoblotting analysis: (1) vector only, (2) WT TM-CD13, (3) L17P TM-CD13, (4) V18P TM-CD13, or (5) I20P TM-CD13. Lanes 6–9 are the same cell lysates treated with *N*-glycosidase F. (B) The culture medium were concentrated, followed by immunoblotting analysis. The loading sequence is the same as in (A). Lane 6 is the control: total cell lysates from cells transfected with the WT TM-CD13 plasmid. (C) Cellular localization of DPP-IV-TM-CD13 detected by cell-surface biotinylation followed by immunoprecipitation. The loading sequence is the same as in (B). Lane 6 is the control: total cell lysates from cells transfected with the WT TM-CD13 plasmid. (D) *In vitro* translation of DPP-IV TM-CD13s in the rabbit reticulocyte lysate system in the presence or absence of rough microsomes (RM). Treatment with proteinase K is indicated. The radioactive proteins were detected by autoradiography.

Anchoring Defects Are Independent of TM Orientation. The TMD of DPP-IV has an N_{in}–C_{out} orientation. To investigate the anchoring capacities of these proline mutant TMDs in the opposite orientation, we fused the DPP-IV TMD after the second TMD of the *Escherichia coli* leader peptidase (Lep) protein[11] and between its two potential glycosylation sites (Figure 9A). In this fusion construct, TM1 of Lep is the membrane targeting sequence. This assay evaluates the membrane integration capacity but not the membrane targeting function of DPP-IV TMs. If inserted into the membrane, the TMD of DPP-IV will be oriented N_{out}–C_{in}, and one

dx.doi.org/10.1021/bi200605h | *Biochemistry* 2011, 50, 7909–7918

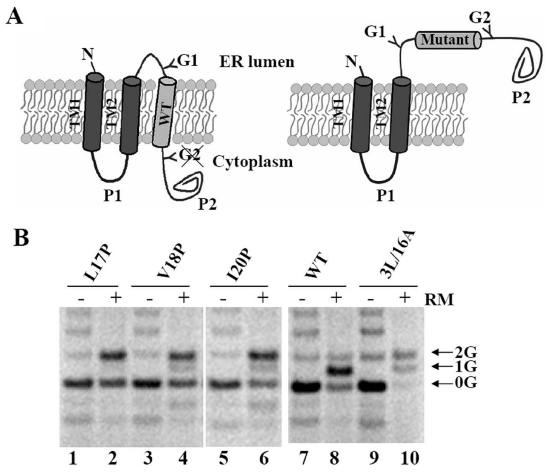

Figure 9. Defective membrane anchoring is independent of TM orientation in the membrane. (A) Lep-DPP-IV fusion constructs. The DPP-IV TMD was fused after the second TMD of the Lep construct. (B) The plasmids encoding the DPP-IV TM-Lep constructs were transcribed and translated in the presence or absence of rough microsomes (RM) in a rabbit reticulocyte lysate system. As the control, a well-characterized Lep/H-segment construct containing three Leu and 16 Ala (3 L/16A) residues was included in the analysis. The radioactive proteins were detected by autoradiography.

glycosylation form (1G) will be detected (Figure 9A); if it is not inserted into the membrane, both the G1 and G2 sites will be glycosylated (2G), distinguishable from the one glycosylation form (1G) on SDS-PAGE (Figure 9A). With WT DPP-IV-Lep, the 1G form of the fusion protein was detected, indicating the membrane insertion of WT TMD (Figure 9B, lane 8). Doubly glycosylated (2G) L17P-Lep, V18P-Lep, and I20P-Lep fusion proteins were detected, indicating that all three mutant TMDs failed to integrate into the membrane (Figure 9B, lanes 2, 4, and 6). The results were consistent with the behaviors of the full-length proteins in intact cells (Figure 2B) and *in vitro* translation experiments (Figures 2 and 3). The orientation of the DPP-IV TMDs in this assay, $N_{out}-C_{in}$, is opposite to the $N_{in}-C_{out}$ of the full-length proteins, indicating that the orientation of the TMDs did not affect their membrane anchoring. Very small amounts of single-glycosylated (1G) V18P-Lep and I20P-Lep fusion proteins were detected, suggesting that small amounts of these two proteins were translocated and integrated into the membrane (Figure 9B, lanes 4 and 6). Whether the integration was due to the presence of Lep TMs in this construct is not clear at this stage.

DISCUSSION

Because proline residues in TMDs play specific and critical roles in the structure and function of many membrane proteins, it is important to understand how they affect the translocation and integration of the proteins into the membrane. In this study, using proline-scanning mutagenesis, we investigated how proline-containing TMDs mediate membrane targeting and integration, with a type II, single-TMD-containing membrane protein DPP-IV.

Our results show that membrane translocation and integration of the TMD are determined by the location and conformation of proline. Three mutant TMDs, L17P, V18P, and I20P, were defective to varying extents in their translocation to the ER and their integration into the membrane (Figures 2 and 3). L17P showed the most severe defect in translocation, failing to translocate at all. Like TMD-less DPP-IV, no protein was detected for L17P in either the cell lysates or the medium, probably because it was rapidly degraded in the cytoplasm. In contrast, the V18P and I20P mutant TMDs were capable of translocating the proteins to the extracellular milieu; however, they failed to anchor the proteins to the membrane. It might not be coincidental that these three proline residues are present in the central and not the N-terminal TMD. The data provide evidence in the context of an endogenous protein that proline has a more drastic effect on membrane targeting and anchoring if it is present in the central region of the TMD. Substitution of proline with Asn, Gln, and His, which have similar hydrophobicity to proline, rescued their translocation defects (Figure 4). Substitution of proline with Gly and Thr, which can modulate the conformation of TM helices, also rescued the translocation defects (Figure 4). Therefore, the conformational change caused by proline, but not its hydrophobicity, is the cause of the detrimental effect observed with membrane translocation and integration.

Our results show that translocation and integration defects of the TMD can be rescued by increasing hydrophobicity through substitutions with more hydrophobic residues in the TMD. Interestingly, the rescue is most effective if these hydrophobic residues are located in the C-terminal part instead of the N-terminal part of the TMD. We showed that T19I or T21I was consistently more effective in rescuing the deficiency of proline substitution in the TMD than G10I, G13I, or even G10I/G13I double substitutions (Figure 7). It is intriguing that it is not the overall hydrophobicity of the TMD that matters, but the localized increase in hydrophobicity. It is not clear mechanistically how hydrophobicity in the vicinity of proline helps to improve the capacity of the TMD to translocate and integrate.

The crystal structure of the protein-conducting channel shows that the lateral gate can accommodate about two helical turns of the TMD for lateral partitioning into the lipid.[2] Adoption of α-helical structure in the membrane translocon is important for efficient membrane insertion.[11,18] Why do the L17P, V18P, and I20P mutations have the most dramatic effects on TMD translocation and integration relative to other mutants? Other than the fact that these three proline mutations are located in the central region of the TMD, the results may be attributable to the second proline at position 24 (P24), which is roughly one or two helical turns away from the first proline. If an α-helix is formed in the DPP-IV TMD, P24 and one of the mutant proline residues would be in the same helical face. If DPP-IV TMD forms α-helices, position 24 would hydrogen-bond with position 20, while position 17 would bond with position 13. With a proline at position 24 and substitution at any of these three positions, the hydrogen-bonding patterns might be disrupted in not only one turn of the helix but in the adjacent turn as well. In addition, proline generally induces a significant kink in TM helices in the membrane environment.[28,40,41] Previously, we have analyzed over 800 TM structures deposited in the Protein Data Bank (PDB).[28] Proline-containing TMs are twice as likely as non-proline-containing TMs to have a kink angle of 20°−45°, whereas non-proline-containing TMs generally have kinks around 5°−20°. For some proline-containing TMs, the kink angles could be as large as 45°−120°.[28] Therefore, the conformation of the DPP-IV TMD might be largely distorted by the presence of additional proline residues. On the basis of our results, we speculate that

because of the structural constraints, two proline residues in the same helical face disrupt the formation of the α-helix by bending the backbone of the TM helix and distorting the hydrogen bonding there. Thus, the canonical helical formation of the TMD might be disrupted, and the interaction with the translocon might be compromised. Consequently, the TMD might not interact with the translocon and might not be translocated or/and integrated properly. Thus, the structure requires a larger amount of energy to pass through the lateral gate of the protein-conducting channel, greatly impeding the integration of the TMD into the membrane, its partitioning to the lipid, or its anchoring to the membrane. Consistent with this hypothesis, the translocation and integration defects could be rescued by either mutating P24 or increasing the hydrophobicity of nearby residues (Figures 6 and 7). Moreover, the capacity of TMD-mediated membrane translocation is largely independent of the extracellular domain and TM orientation, indicating that the interaction between the TMD and the translocon is the key determinant for a successful protein translocation.

The ΔG_{app} scale is successful in predicting the translocation behavior of single-span non-proline-containing TMDs.[11,12] How this scale predicts the behavior of endogenous proteins under intact cell culture conditions is unknown. The scale predicted that all three mutants (L17P, V18P, and I20P, all with P24) would have unfavorable ΔG_{app} values and would not be translocated or integrated (Supporting Information Figure 2A). It also predicted that the I21P mutant would not be translocated (Supporting Information Figure 2A). However, our experimental data indicate that the V18P and I20P mutants translocated their TMDs correctly but did not anchor them (Figures 2 and 3), whereas the I21P mutant was translocated and anchored properly (Figure 2B). The scale partially correctly predicts the translocation behavior of TMDs with G/T substitutions at L17, V18, and I20 (Supporting Information Figure 2B) but fails to predict the translocation behavior of TMDs with N/Q/H substitutions at these positions (Supporting Information Figure 2B). Based on our results, the conformation of the TMD, the position of proline, and its TM sequence context are critical factors to be considered when the insertional efficiency of a protein is calculated. The conformational change of the TMD in the presence of proline depends on its location in the TMD,[42,43] which might explain why the I20P mutant is the most difficult to fully rescue by either substitution with another amino acid or increasing the hydrophobicity in the nearby region (Figures 4 and 7). It has been shown that a pair of proline residues separated by 4−10 residues maximally reduces the efficiency of membrane insertion.[12] Our results suggest that the distance between the pair of proline residues is not the determining factor. In the two-proline mutants studied here, it was not simply the distance between the two proline residues that governed the membrane translocation and integration of the TMD. Instead, the translocation and integration were TMD-sequence dependent. The location of proline affects the local structure of the TMD. As a result, the interaction of the TMD with the translocon might be affected, resulting in different translocation and anchoring behaviors. How proline affects the translocation and membrane integration of a protein remains an interesting question to be further investigated.

■ ASSOCIATED CONTENT

Ⓢ Supporting Information

Mutant DPP-IV proteins were localized on the plasma membrane and they maintained their dimeric structures (Figure 1S), apparent free energy ΔG_{app} scale of mutant DPP-IV TMDs (Figure 2S), and the primer sequences for the mutations generated in this study (Table 1S). This material is available free of charge via the Internet at http://pubs.acs.org.

■ AUTHOR INFORMATION

Corresponding Author

*Tel: 886 37 246166 ext 35718. Fax: 886 37 586456. E-mail: xchen@nhri.org.tw.

Funding

This study was supported by NRPGM, National Science Council, and National Health Research Institutes, Taiwan, ROC, to X.C. and NSC-95-3114-P-002-005-Y to M.-J.H.

■ ACKNOWLEDGMENTS

We thank Dr. Gunnar von Heijne for reading the manuscript and giving suggestions and Drs. Tom Rapoport and Hsou-Min Li for discussions and suggestions. We also thank Ms. Hsiang-Yun Tang for her technical assistance.

■ ABBREVIATIONS

ER, endoplasmic reticulum; TM, transmembrane; TMD, transmembrane domain; SRP, signal recognition particle; ΔG_{app}, the apparent free energy; DPP-IV, dipeptidyl peptidase-IV; Pro, proline; CHO, Chinese hamster ovary cells; WT, wild type; sulfo-NHS-biotin, *N*-hydroxysulfosuccinimidobiotin; PBS, phosphate-buffered saline; Lep, leader peptidase.

■ REFERENCES

(1) Rapoport, T. A. (2007) Protein translocation across the eukaryotic endoplasmic reticulum and bacterial plasma membranes. *Nature 450*, 663−669.

(2) Osborne, A. R., Rapoport, T. A., and van den Berg, B. (2005) Protein translocation by the Sec61/SecY channel. *Annu. Rev. Cell Dev. Biol. 21*, 529−550.

(3) Cannon, K. S., Or, E., Clemons, W. M. Jr., Shibata, Y., and Rapoport, T. A. (2005) Disulfide bridge formation between SecY and a translocating polypeptide localizes the translocation pore to the center of SecY. *J. Cell Biol. 169*, 219−225.

(4) Heinrich, S. U., Mothes, W., Brunner, J., and Rapoport, T. A. (2000) The Sec61p complex mediates the integration of a membrane protein by allowing lipid partitioning of the transmembrane domain. *Cell 102*, 233−244.

(5) Mothes, W., Heinrich, S. U., Graf, R., Nilsson, I., von Heijne, G., Brunner, J., and Rapoport, T. A. (1997) Molecular mechanism of membrane protein integration into the endoplasmic reticulum. *Cell 89*, 523−533.

(6) Plath, K., Mothes, W., Wilkinson, B. M., Stirling, C. J., and Rapoport, T. A. (1998) Signal sequence recognition in posttranslational protein transport across the yeast ER membrane. *Cell 94*, 795−807.

(7) Wimley, W. C., Creamer, T. P., and White, S. H. (1996) Solvation energies of amino acid side chains and backbone in a family of host-guest pentapeptides. *Biochemistry 35*, 5109−5124.

(8) Wimley, W. C., Gawrisch, K., Creamer, T. P., and White, S. H. (1996) Direct measurement of salt-bridge solvation energies using a peptide model system: implications for protein stability. *Proc. Natl. Acad. Sci. U. S. A. 93*, 2985−2990.

(9) Wimley, W. C., and White, S. H. (1996) Experimentally determined hydrophobicity scale for proteins at membrane interfaces. *Nat. Struct. Biol. 3*, 842−848.

(10) Jayasinghe, S., Hristova, K., and White, S. H. (2001) Energetics, stability, and prediction of transmembrane helices. *J. Mol. Biol. 312*, 927−934.

(11) Hessa, T., Kim, H., Bihlmaier, K., Lundin, C., Boekel, J., Andersson, H., Nilsson, I., White, S. H., and von Heijne, G. (2005) Recognition of transmembrane helices by the endoplasmic reticulum translocon. *Nature 433*, 377−381.

(12) Hessa, T., Meindl-Beinker, N. M., Bernsel, A., Kim, H., Sato, Y., Lerch-Bader, M., Nilsson, I., White, S. H., and von Heijne, G. (2007) Molecular code for transmembrane-helix recognition by the Sec61 translocon. *Nature 450*, 1026−1030.

(13) White, S. H., and von Heijne, G. (2008) How translocons select transmembrane helices. *Annu. Rev. Biophys. 37*, 23−42.

(14) Brandl, C. J., and Deber, C. M. (1986) Hypothesis about the function of membrane-buried proline residues in transport proteins. *Proc. Natl. Acad. Sci. U. S. A. 83*, 917−921.

(15) Senes, A., Engel, D. E., and DeGrado, W. F. (2004) Folding of helical membrane proteins: the role of polar, GxxxG-like and proline motifs. *Curr. Opin. Struct. Biol. 14*, 465−479.

(16) Presta, L. G., and Rose, G. D. (1988) Helix signals in proteins. *Science 240*, 1632−1641.

(17) Richardson, J. S., and Richardson, D. C. (1988) Amino acid preferences for specific locations at the ends of alpha helices. *Science 240*, 1648−1652.

(18) Lundin, C., Kim, H., Nilsson, I., White, S. H., and von Heijne, G. (2008) Molecular code for protein insertion in the endoplasmic reticulum membrane is similar for Nin-Cout and Nout-Cin transmembrane helices. *Proc. Natl. Acad. Sci. U. S. A.*, .

(19) Yohannan, S., Yang, D., Faham, S., Boulting, G., Whitelegge, J., and Bowie, J. U. (2004) Proline substitutions are not easily accommodated in a membrane protein. *J. Mol. Biol. 341*, 1−6.

(20) Deacon, C. F., Ahren, B., and Holst, J. J. (2004) Inhibitors of dipeptidyl peptidase IV: a novel approach for the prevention and treatment of Type 2 diabetes. *Expert Opin. Investig. Drugs 13*, 1091−1102.

(21) Hong, W. J., and Doyle, D. (1988) Membrane orientation of rat gp110 as studied by in vitro translation. *J. Biol. Chem. 263*, 16892−16898.

(22) Low, S. H., Tang, B. L., Wong, S. H., and Hong, W. (1994) Golgi retardation in Madin-Darby canine kidney and Chinese hamster ovary cells of a transmembrane chimera of two surface proteins. *J. Biol. Chem. 269*, 1985−1994.

(23) Munro, S. (1991) Sequences within and adjacent to the transmembrane segment of alpha-2,6-sialyltransferase specify Golgi retention. *EMBO J. 10*, 3577−3588.

(24) Hong, W. J., and Doyle, D. (1990) Molecular dissection of the NH2-terminal signal/anchor sequence of rat dipeptidyl peptidase IV. *J. Cell Biol. 111*, 323−328.

(25) Chien, C. H., Huang, L. H., Chou, C. Y., Chen, Y. S., Han, Y. S., Chang, G. G., Liang, P. H., and Chen, X. (2004) One site mutation disrupts dimer formation in human DPP-IV proteins. *J. Biol. Chem. 279*, 52338−52345.

(26) Chien, C. H., Tsai, C. H., Lin, C. H., Chou, C. Y., and Chen, X. (2006) Identification of hydrophobic residues critical for DPP-IV dimerization. *Biochemistry 45*, 7006−7012.

(27) Conarello, S. L. (2003) Mice lacking dipeptidyl peptidase IV are protected against obesity and insulin resistance. *Proc. Natl. Acad. Sci. U. S. A. 100*, 6825−6830.

(28) Chung, K.-M., Cheng, J.-H., Suen, C.-S., Huang, C.-H., Tsai, C.-H., Huang, L.-H., Chen, Y.-R., Wang, A. H. J., Jiaang, W.-T., Hwang, M.-J., and Chen, X. (2010) The dimeric transmembrane domain of prolyl dipeptidase DPP-IV contributes to its quaternary structure and enzymatic activities. *Protein Sci. 19*, 1627−1638.

(29) Pacheco, R. (2005) CD26, adenosine deaminase, and adenosine receptors mediate costimulatory signals in the immunological synapse. *Proc. Natl. Acad. Sci. U. S. A. 102*, 9583−9588.

(30) Dong, R. P., and Morimoto, C. (1996) Role of CD26 for CD4 memory T cell function and activation. *Hum. Cell 9*, 153−162.

(31) Lee, H. J., Chen, Y. S., Chou, C. Y., Chien, C. H., Lin, C. H., Chang, G. G., and Chen, X. (2006) Investigation of the Dimer Interface and Substrate Specificity of Prolyl Dipeptidase DPP8. *J. Biol. Chem. 281*, 38653−38662.

(32) Chen, X., Wen, S., Fukuda, M. N., Gavva, N. R., Hsu, D., Akama, T. O., Yang-Feng, T., and Shen, C. K. (2001) Human ITCH is a coregulator of the hematopoietic transcription factor NF-E2. *Genomics 73*, 238−241.

(33) Hurley, W. L., and Finkelstein, E. (1990) Identification of leukocyte surface proteins. *Methods Enzymol. 184*, 429−433.

(34) Bourd-Boittin, K., Le Pabic, H., Bonnier, D., L'Helgoualc'h, A., and Theret, N. (2008) RACK1, a new ADAM12 interacting protein. Contribution to liver fibrogenesis. *J. Biol. Chem. 283*, 26000−26009.

(35) Fazio, S., Horie, Y., Weisgraber, K. H., Havekes, L. M., and Rall, S. C. Jr. (1993) Preferential association of apolipoprotein E Leiden with very low density lipoproteins of human plasma. *J. Lipid Res. 34*, 447−453.

(36) Tang, H. K., Tang, H. Y., Hsu, S. C., Chu, Y. R., Chien, C. H., Shu, C. H., and Chen, X. (2009) Biochemical properties and expression profile of human prolyl dipeptidase DPP9. *Arch. Biochem. Biophys. 485*, 120−127.

(37) He, M., and Taussig, M. J. (1997) Antibody-ribosome-mRNA (ARM) complexes as efficient selection particles for in vitro display and evolution of antibody combining sites. *Nucleic Acids Res. 25*, 5132−5134.

(38) Ballesteros, J. A., Deupi, X., Olivella, M., Haaksma, E. E., and Pardo, L. (2000) Serine and threonine residues bend alpha-helices in the chi(1) = g(-) conformation. *Biophys. J. 79*, 2754−2760.

(39) Deupi, X., Olivella, M., Govaerts, C., Ballesteros, J. A., Campillo, M., and Pardo, L. (2004) Ser and Thr residues modulate the conformation of pro-kinked transmembrane alpha-helices. *Biophys. J. 86*, 105−115.

(40) Senes, A., Engel, D. E., and DeGrado, W. F. (2004) Folding of helical membrane proteins: the role of polar, GxxxG-like and proline motifs. *Curr. Opin. Struct. Biol. 14*, 465−479.

(41) Cordes, F. S., Bright, J. N., and Sansom, M. S. P. (2002) Proline-induced Distortions of Transmembrane Helices. *J. Mol. Biol. 323*, 951−960.

(42) Nilsson, I., Saaf, A., Whitley, P., Gafvelin, G., Waller, C., and von Heijne, G. (1998) Proline-induced disruption of a transmembrane alpha-helix in its natural environment. *J. Mol. Biol. 284*, 1165−1175.

(43) Nilsson, I., and von Heijne, G. (1998) Breaking the camel's back: proline-induced turns in a model transmembrane helix. *J. Mol. Biol. 284*, 1185−1189.